Stability of dissipative optical solitons in the three-dimensional cubic-quintic Ginzburg-Landau equation

D. Mihalache,[1] D. Mazilu,[1] F. Lederer,[2] H. Leblond,[3] and B. A. Malomed[4]
[1]*Horia Hulubei National Institute for Physics and Nuclear Engineering (IFIN-HH), 407 Atomistilor, Magurele-Bucharest, 077125, Romania*
[2]*Institute of Solid State Theory and Theoretical Optics, Friedrich-Schiller Universität Jena, Max-Wien-Platz 1, D-077743 Jena, Germany*
[3]*Laboratoire POMA, UMR 6136, Université d'Angers, 2 Bd Lavoisier, 49000 Angers, France*
[4]*Department of Interdisciplinary Studies, Faculty of Engineering, Tel Aviv University, Tel Aviv 69978, Israel*
(Received 17 January 2007; published 23 March 2007)

We report results of a systematic analysis of the stability of dissipative optical solitons, with intrinsic vorticity $S=0$ and 1, in the three-dimensional complex Ginzburg-Landau equation with the cubic-quintic nonlinearity, which is a model of a dispersive optical medium with saturable self-focusing nonlinearity and bandwidth-limited nonlinear gain. The stability is investigated by means of computation of the instability growth rate for eigenmodes of small perturbations, and the results are verified against direct numerical simulations. We conclude that the presence of diffusivity in the transverse plane is necessary for the stability of vortex solitons (with $S=1$) against azimuthal perturbations, while zero-vorticity solitons may be stable in the absence of the diffusivity. On the other hand, the solitons with $S=0$ and $S=1$ have their stability regions at both anomalous and normal group-velocity dispersion, which is important to the experimental implementation. At values of the nonlinear gain above their existence region, the solitons either develop persistent intrinsic pulsations, or start expansion in the longitudinal direction, keeping their structure in the transverse plane.

DOI: 10.1103/PhysRevA.75.033811 PACS number(s): 42.65.Tg, 42.65.Sf, 47.20.Ky

I. INTRODUCTION

Solitons, which are represented by localized solutions of nonlinear partial differential equations [1], are ubiquitous self-supporting objects found in media of very different physical nature. Among various realizations of solitons in fundamental and applied physics, especially important are those in nonlinear optics [2–7]. In integrable systems, which provide for a strongly idealized description of physical media, the solitons preserve their shape upon interaction and may be viewed as "nonlinear modes" of the corresponding model. In more realistic nonintegrable systems (conservative or dissipative ones), solitons (or, strictly speaking, *solitary waves*) may also be regarded as nonlinear modes, even if their properties are different from those of their counterparts in integrable models. In conservative media, the solitary waves are supported by stable balance between diffraction and/or dispersion and nonlinearity, whereas, in the presence of dissipation, gain and loss must also be balanced. In the former situation, solitons (in integrable and nonintegrable models alike) form continuous families with one or more intrinsic parameters, whereas in the latter case the condition of the balance between gain and loss results in a solitary-wave solution [*dissipative soliton* (DS) [8–10]] having its amplitude and velocity fixed by coefficients of the governing equations, i.e., stationary soliton solutions are isolated ones.

A necessary condition for the full stability of a DS is the stability of its background, i.e., zero solution. Therefore, the systems supporting stable DSs are necessarily *bistable*, featuring two competing *attractors*: The DS itself, and the zero solution. A border between their attraction basins is a *separatrix*, which is represented by an additional *unstable* DS. Thus stable DSs may only appear in pairs with their unstable counterparts. Known examples of models that feature such solution pairs, available in an exact analytical form, are the one-dimensional (1D) nonlinear Schrödinger (NLS) equation which includes linear loss and parametric-gain terms [11], and a system of linearly coupled 1D cubic and linear complex Ginzburg-Landau (CGL) equations [12]. Contrary to that, models admitting a single DS solution, such as the cubic CGL equation *per se* [13], do not give rise to stable pulses.

Generally, CGL equations are universal models to describe the dynamics of dissipative physical media close to the onset of pattern-forming instabilities [14–16]. In this and related capacities, the CGL equations find applications in diverse branches of physics, such as superconductivity, fluid dynamics, plasmas, chemical-reaction waves, nonlinear optics, and others [14–17]. In addition to the above-mentioned DSs (alias solitary pulses), these equations give rise to solutions of other kinds, such as shocks, sources, sinks, and various pulsating states. These solutions describe physically significant patterns in laser cavities [18], hydrodynamic flows [19], nonlinear optics [17,20–22], and hot plasmas [13,23].

A model which supports stable DSs and is more generic than the above-mentioned specific ones (based on the damped parametrically driven NLS equation [11], or the system of coupled cubic and linear CGL equations [12,24]), is provided by an equation of the CGL type with the cubic-quintic (CQ) nonlinearity. Note that the CQ nonlinearity is a quite generic one in both optical and atomic systems (for a recent study of a four-level atomic system with electromagnetically induced transparency with giant CQ nonlinearities of opposite signs, see Ref. [25]). The CGL equation with CQ nonlinearities was first introduced, in the 2D form, by Petviashvili and Sergeev [26], and later considered in many other

 ©2007 The American Physical Society

papers; see, e.g., Refs. [24,27–31] and references therein. In addition to stationary solitary pulses, more sophisticated solutions to the CQ CGL equations in one dimension, such as exploding (erupting) solitons and fronts [32], and "creeping solitons" [33], were found too.

The CGL equation with the CQ nonlinearity makes it possible to find stable localized solutions in the 2D and 3D geometry. In particular, stable 2D states in the form of spiral solitons (ones with "spin," i.e., intrinsic vorticity, $S=1$ and 2) were found by means of numerical methods in Refs. [34]. Stable DS solutions in three dimensions, which resemble "light bullets," i.e., 3D (spatiotemporal) solitons, which were predicted in several conservative models of nonlinear optics, but have not yet been created in the experiment [6], were reported recently, for both anomalous and normal group-velocity dispersion (GVD) [35,36] (anomalous GVD is a necessary condition for the existence of solitons in any conservative model in any dimension [6], while stable solitary pulses were found before in 1D dissipative models with normal GVD [37]). In the case when the domination of the normal GVD does not allow the existence of DSs, the process of the temporal elongation of 3D pulses into expanding "rockets" was investigated too [36]. Another issue of interest is a possibility to form complexes ("molecules") of solitons in dissipative systems. In particular, the concept of an "optical soliton molecule" was introduced to describe quasistable aggregates of solitons in 3D conservative models [38]. However, such "molecules" in conservative media are subject to gradual decay on a long propagation scale.

An especially challenging problem is the stability of 3D solitons with intrinsic vorticity (alias *vortex tori*, so called due to their doughnutlike shape), against both the supercritical collapse in the 3D space, caused by the self-focusing nonlinearity, and the specific *splitting instability* of vortical solitons [6,39,40]. Stable 3D solitons with spin (alias topological charge) $S=1$ were found in conservative models that, to arrest the collapse, rely on competing nonlinearities, such as cubic-quintic or quadratic-cubic [40]. Stability of localized vortices was also explored in the 3D Gross-Pitaevskii equation with the self-attractive cubic nonlinearity and an isotropic trapping potential [41]. It is also relevant to mention that many types of stable 3D solitons with intrinsic vorticity were found in the discrete NLS equation with the cubic nonlinearity [42]. In the context of 3D vortical-soliton states, remaining issues are the stability of multicharged vortex tori with $S>1$ (stable higher-order vortex solitons were found in 2D models [43,44]), and the search for stable vortical solitons in 3D dissipative media. The above-mentioned results of Ref. [34], where stable 2D vortex solitons, with a spiral phase field, were found for $S=1$ and 2, suggest that the CQ CGL equation may be a relevant model to generate vortex DSs in the 3D case too. Indeed, stable 3D spinning solitons (vortex tori), with both $S=1$ and $S=2$, have been reported in this model [45]. Those results present not only the first species of stable spinning solitons in a 3D dissipative medium, but also the first example of stable higher-order ($S>1$) vortex solitons in *any* 3D model. In addition, stable fundamental, alias spinless ($S=0$), 3D spatiotemporal solitons [35,36,46], as well as double-soliton complexes, including rotating ones [47], have been found in an optical model based on the CQ CGL equation.

The aim of this paper is to explore physically significant properties of the 3D solitons in the CGL model with the CQ nonlinearity. In particular, our objective is to find out what ingredients of the model are crucial to the stability of the spinless and spinning solitons. In this connection, it is necessary to mention that the underlying equation features the CQ nonlinearity in both its conservative and dissipative parts; see Eq. (1) below. As mentioned above, in conservative models, such as the CQ NLS equation, the quintic self-defocusing term is necessary to suppress the supercritical collapse, the trend to which is caused, in the 3D space, by the self-focusing cubic nonlinearity [6]. In Ref. [45], it has been demonstrated that the saturation of the self-focusing nonlinearity (through the quintic term) in the conservative part of the CGL equation is not necessary for the stability of 3D fundamental and vortex DSs, because the trend to collapse is suppressed by the quintic term in the dissipative part of the equation. However, the results were reported in Ref. [45] only with nonzero diffusivity in the transverse plane, and anomalous GVD in the longitudinal (temporal) direction [$\gamma>0$ and $D>0$ in Eq. (1); see below]. For the experimental creation of the solitons, it is important to know the sensitivity of the stability to these two factors. In particular, setting $\gamma=0$ renders the model Galilean invariant in the transverse directions, which makes it possible to create moving solitons and study collisions between them [48]. The sign of the GVD is important too, as the experiment is usually conducted in a vicinity of the zero-dispersion point of the carrier wavelength; hence both signs are relevant.

In this work, we demonstrate that the diffusivity is indeed necessary for the stability of the vortex solitons against splitting (while the zero-vorticity solitons may be stable in the absence of the diffusivity). We demonstrate too that stable dissipative solitons, with zero and nonzero vorticity alike, exist at both anomalous and normal GVD. In fact, the stability region of vortex dissipative solitons is *larger* in the latter case, which suggests that the solitons may be created in an expanded range of the carrier wavelength (on both sides of the zero-dispersion point). In addition, we demonstrate that, at values of the nonlinear gain above the upper border of the existence region for stationary 3D dissipative solitons, they start either intrinsic pulsations, or permanent expansion in the temporal (longitudinal) direction, while keeping their structure in the transverse plane.

The paper is organized as follows: After introducing the CQ CGL model in Sec. II, in Sec. III we report results of systematic analysis demonstrating the existence and stability of both spinless and spinning solitons in both the normal- and anomalous-GVD regimes. Stability borders for these states are accurately delineated. Direct numerical simulations of the evolution of perturbed solutions show full agreement with predictions based on computation of instability eigenvalues from the linearized equations for small perturbations. The paper is concluded by Sec. IV.

II. CUBIC-QUINTIC GINZBURG-LANDAU MODEL

We consider a model of a bulk (3D) optical medium described by the following equation for a local amplitude, U, of

the electromagnetic field propagating along axis z [35,36,45,46]:

$$iU_z + \left(\frac{1}{2} - i\beta\right)(U_{xx} + U_{yy}) + \left(\frac{D}{2} - i\gamma\right)U_{tt} + [i\delta + (1 - i\varepsilon)|U|^2 - (\nu - i\mu)|U|^4]U = 0. \quad (1)$$

Here, the coefficients which are scaled to be 1/2 and 1 account, respectively, for the diffraction in transverse plane (x,y) and the self-focusing Kerr nonlinearity, $\beta \geqslant 0$ is the above-mentioned effective diffusivity in the transverse plane (the optical model contains the diffusion term if the electromagnetic field generates free carriers, which may occur in semiconductor waveguides [34,49], or ionizes the medium, which happens in the case of the propagation of very strong pulses in air [50]). A CGL model including a spatial diffusion term has also been derived from the Maxwell-Bloch equations, in the case of a laser in the bad cavity configuration [51]. Variants of this model of Swift-Hohenberg type [52] or involving two contrapropagating waves [53] relate the constant β to the laser detuning. Further, positive parameters δ, ε, and μ represent, respectively, the linear loss, nonlinear gain, and its saturation, which are ordinary ingredients of the CQ CGL equation [26]; $\nu \geqslant 0$ accounts for the above-mentioned self-defocusing quintic correction to the Kerr term (saturation of the optical nonlinearity). Notice that nonzero quintic nonlinear terms may arise in a laser cavity even if the susceptibility $\chi^{(5)}$ of the optical materials used is negligible. This has been demonstrated in the 1D case of a fiber laser mode-locked by nonlinear rotation of the polarization [54]; however, ν was zero in this situation. D is the GVD coefficient ($D<0$ and $D>0$ correspond to the normal and anomalous dispersion), and $\gamma>0$ is its counterpart accounting for the spectral filtering, i.e., bandwidth-limited character of the gain.

Solutions to Eq. (1) in the form of vortical DSs are looked for as

$$U(z,x,y,t) = \Psi(z,r,t)\exp(iS\theta), \quad (2)$$

where r and θ are the polar coordinates in plane (x,y), S is the above-mentioned integer spin (vorticity), and complex function $\Psi(z,r,t)$ obeys the propagation equation

$$i\Psi_z + \left(\frac{1}{2} - i\beta\right)\left(\Psi_{rr} + \frac{1}{r}\Psi_r - \frac{S^2}{r^2}\Psi\right) + \left(\frac{1}{2}D - i\gamma\right)\Psi_{tt} + [i\delta + (1 - i\varepsilon)|\Psi|^2 - (\nu - i\mu)|\Psi|^4]\Psi = 0 \quad (3)$$

(due to the complexity of Ψ, the intrinsic phase fields of the vortical solitons has the form of rotating spirals in the transverse plane [34]). Solutions to Eq. (3) must decay exponentially at $r,|t| \to \infty$, and as $r^{|S|}$ at $r \to 0$.

To find relevant solutions, we simulated Eq. (3) forward in z, starting with an arbitrary axially symmetric input pulse (typically, a Gaussian) corresponding to vorticity S, in the form of

$$\Psi_0(r,t) = A_0 r^S \exp\left[-\frac{1}{2}\left(\frac{r^2}{r_0^2} + \frac{t^2}{t_0^2}\right)\right],$$

with real constants A_0, r_0, t_0, in anticipation of self-trapping of the pulse into a stable DS (*attractor*). The thus found established DS can be eventually represented in the form of

$$\Psi(z,r,t) = \psi(r,t)\exp(ikz), \quad (4)$$

where propagation constant k is, as a matter of fact, an eigenvalue determined by parameters of Eq. (3) (including S). A standard Crank-Nicholson scheme of the numerical integration was used, with typical transverse and longitudinal step sizes $\Delta r = \Delta t = 0.1$ and $\Delta z = 0.005$. The nonlinear finite-difference equations were solved by dint of the Picard iteration method, and the resulting linear system was then handled with the help of the Gauss-Seidel iterative procedure. To achieve good convergence, ten Picard and four Gauss-Seidel iterations were typically needed. Wave number k was finally found as a value of the z derivative of the phase of $\Psi(z,r,t)$. The solution was reckoned to achieve a stationary form if k ceased to depend on z, r, and t, up to five significant digits.

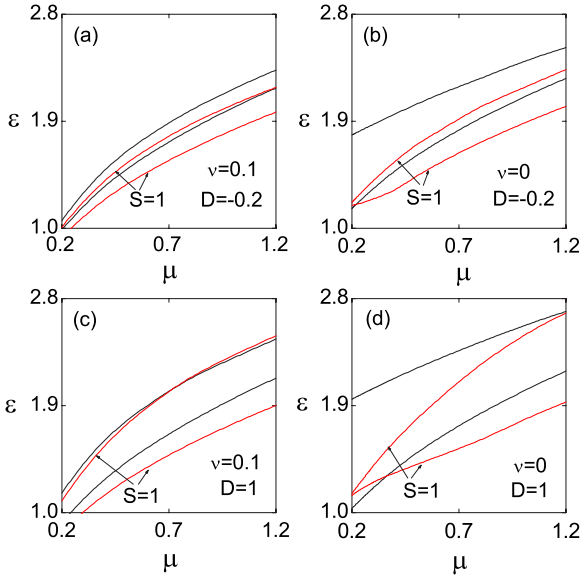

FIG. 1. (Color online) The existence and stability domains of dissipative solitons with $S=0$ and $S=1$ for $\beta=0$ (zero diffusivity) in the plane of the quintic-loss and cubic-gain coefficients, (μ,ε), for (a), (b) normal and (c), (d) anomalous GVD. Other parameters are $\gamma=0.5$ and $\delta=0.4$. The $S=0$ solitons are stable in the domains between black curves. The $S=1$ solitons exist and are *unstable* in the domains between red (dark-gray) curves.

III. SOLITON SOLUTIONS AND THEIR STABILITY

A. Stationary and nonstationary solitons

In Fig. 1 we show the existence and stability domains for spinless ($S=0$) and spinning ($S=1$) DSs in the plane of (μ,ε) [i.e., quintic-loss and cubic-gain coefficients in Eq. (1)] for zero diffusivity, $\beta=0$, and different values of ν and GVD coefficient D, the other parameters being $\gamma=0.5$ and $\delta=0.4$. As might be expected, the existence domains are larger in the case of the anomalous GVD; nevertheless, the solitons exist too with normal GVD. In Fig. 1, the $S=0$ solitons are stable in the entire existence domain between black lines in each

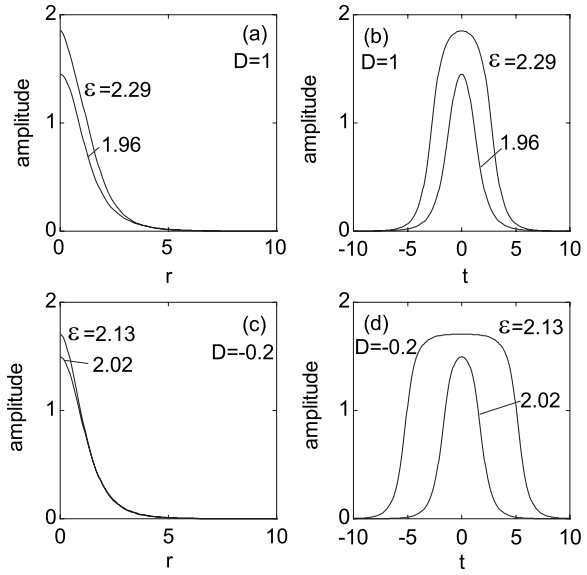

FIG. 2. Cross-section shapes of typical stable solitons with $S=0$ in the transverse (r) and temporal (t) directions, for values of D and ε indicated in the panels, including cases of (a), (b) anomalous and (c), (d) normal GVD. Other parameters are $\beta=0$, $\mu=1$, and $\nu=0.1$.

panel, whereas the $S=1$ vortex solitons exist and are *always unstable* (recall that the results in Fig. 1 pertain to the zero value of diffusivity β) in regions between red (dark-gray) curves in each panel (a)–(d) (details of the linear stability analysis for these solutions are presented below). Beneath the lower curves in each panel of Fig. 1, the input pulses corresponding to $S=0$ and $S=1$ decay to nil, whereas above the upper borders they either feature nearly periodic evolution, converging to *pulsating solitons* (breathers), spinless or spinning ones (see below), or expand indefinitely in the time domain but remain localized in the spatial domain (see below too). Note that the stable solitons (ones with $S=0$, in this case) are *strong attractors*, as they self-trap from a large variety of inputs.

Typical radial and temporal cross sections of stable solitons with $S=0$ and $S=1$ are shown in Figs. 2(a)–2(d) for $\beta=0$, $\mu=1$, $\nu=0.1$, and two representative values of ε, in both the normal- and anomalous-GVD regimes. In the case of the normal GVD and for large values of the nonlinear-gain coefficient, ε, near the existence border, the solitons display a characteristic flat-top shape; see panel (d) in Fig. 2.

As mentioned above, the spinning and spinless DSs may continue to exist above the upper borders in Fig. 1, but in the form of pulsating, rather than stationary, solitons. To illustrate this point, in Fig. 3 we show the total energy of a pulsating vortex soliton with $S=1$,

$$E = \int_0^{\infty} r\,dr \int_0^{2\pi} d\theta \int_{-\infty}^{+\infty} dt |U(r,\theta,t)|^2 \equiv 2\pi \int_0^{\infty} r\,dr \int_{-\infty}^{+\infty} dt |\psi(r,t)|^2 \tag{5}$$

[see Eq. (2)], as a function of propagation distance z, for $\beta=0$, $\nu=0.1$ $\varepsilon=2.05$, $\mu=1$, and normal GVD, $D=-0.2$. Note that this soliton features regular (single-period) shape vibrations, between the cross sections shown in Figs. 3(b) and 3(c). In the case of anomalous GVD, the energy of spinless ($S=0$) and spinning ($S=1$) pulsating solitons is shown, as a function of the propagation distance, in Fig. 4. In this case, contrary to the situation with the normal GVD, the $E(z)$ curves reveal complex (multiple-period) pulsations.

Another possible outcome of the evolution above the upper borders in Fig. 1 is conversion of the soliton into an expanding pattern filling the space between two fronts moving in opposite directions along the temporal axis, while the pattern's shape remains stationary in the (x,y) plane. This possibility is illustrated by Fig. 5, which displays typical cross-section shapes, in the transverse (r) and temporal (t) directions, of the pattern generated, in this case, by an initial zero-vorticity solitary pulse.

The families of the 3D spinless and spinning solitons in the CQ CGL model, and their stability, are represented, in Figs. 6 and 7, by dependences of the soliton's energy on the cubic-gain coefficient, ε, at zero ($\beta=0$) and finite ($\beta=0.1$) values of diffusivity coefficient β. The stability of the solutions was identified through the computation of the instabil-

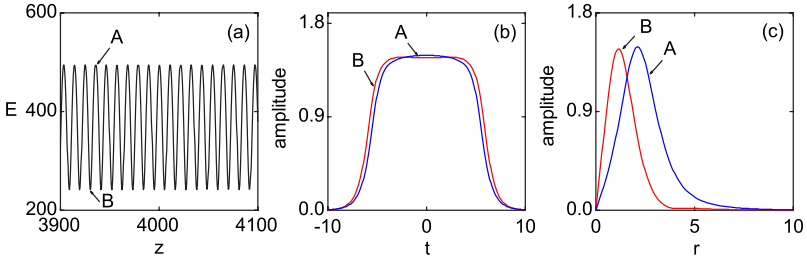

FIG. 3. (Color online) (a) The soliton's energy, defined in Eq. (5), versus the propagation distance for a pulsating vortex dissipative soliton with $S=1$, at $\beta=0$, $\nu=0.1$ $\varepsilon=2.05$, $\mu=1$, and normal GVD, $D=-0.2$. Panels (b) and (c) display the soliton's cross-section shapes in the transverse (r) and temporal (t) directions, at positions with the maximum and minimum energy [points A and B, respectively, in panel (a)], between which the soliton oscillates.

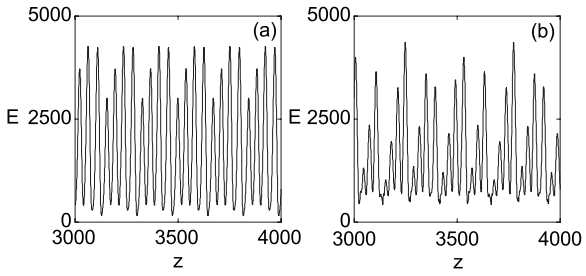

FIG. 4. The soliton's energy versus the propagation distance for pulsating solitons at $\varepsilon=2.33$: (a) $S=0$ and (b) $S=1$. Other parameters are $\beta=0$, $\nu=0.1$, $\mu=1$, and $D=1$ (anomalous GVD).

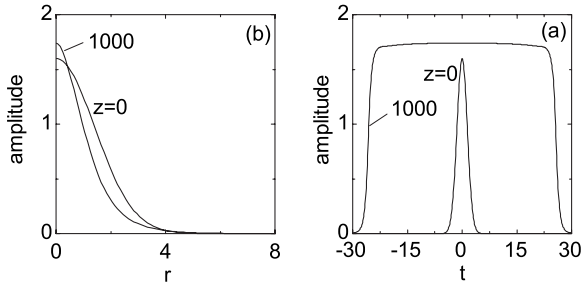

FIG. 5. Typical cross-section shapes in the (a) transverse (r) and (b) temporal (t) directions of the expanding zero-vorticity pattern formed by two fronts running along the temporal direction. Here, $\beta=0, \varepsilon=2.2$, $\nu=0.1$, $\mu=1$, and $D=-0.2$ (normal GVD).

ity growth rate for eigenmodes of small perturbations, as described in detail below.

As mentioned above, the $S=0$ solitons may be stable at zero diffusivity, but all the spinning solitons, with $S=1$, are unstable in this case, while a part of their family is stable, as marked by arrows (stability borders) in Fig. 7, at $\beta=0.1$. It is noteworthy that there is one stability border in the case of normal GVD, Fig. 7(a), and two borders (with the stability region located between them) if the GVD is anomalous, Fig. 7(b). Moreover, although the anomalous character of the GVD is a necessary condition for the existence of solitons in conservative media, we conclude from Fig. 7 (as also confirmed by Fig. 9, see below) that the stability region for the vortex DSs is *larger* in the case of normal GVD than for anomalous chromatic dispersion. On the other hand, the saturation of the self-focusing nonlinearity, accounted for by parameter $\nu \geqslant 0$ in Eq. (1), is *not* crucial to the stability: As seen in Figs. 6 and 7, both the spinless and spinning solitons may be stable at $\nu=0$.

B. Stability analysis: Infinitesimal and finite perturbations

To study the stability of the stationary solitons in an accurate form, a perturbed solution to Eq. (1) was looked for as

$$U = [\psi(r,t) + f(r,t)\exp(\lambda z + iJ\theta) + g^*(r,t)\exp(\lambda^* z - iJ\theta)]\exp(ikz + iS\theta),$$

where $\psi(r,t)$ is the function defined in Eq. (4), J is an integer

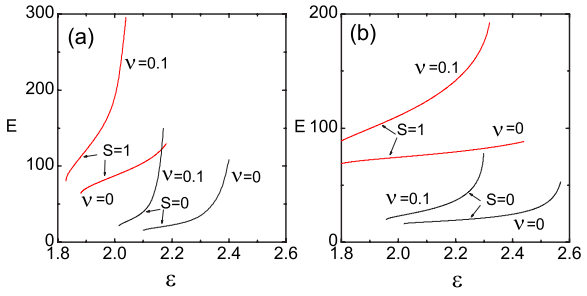

FIG. 6. (Color online) The energy of the nonspinning ($S=0$) and spinning ($S=1$) solitons versus the nonlinear-gain parameter, ε, for zero diffusivity, $\beta=0$, and $\mu=1$: (a) $D=-0.2$ and (b) $D=1$. Here and in Fig. 7, red (dark gray) and black branches (or parts thereof) represent unstable and stable solutions, respectively.

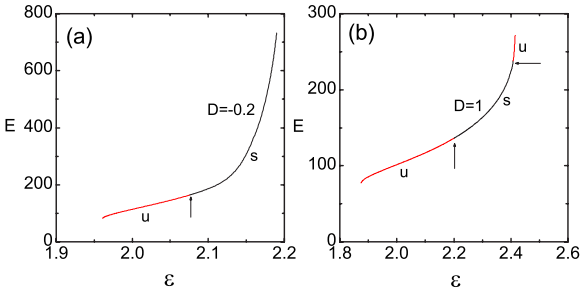

FIG. 7. (Color online) The same as in Fig. 6, but for spinning solitons, with $S=1$, at nonzero diffusivity, $\beta=0.1$. Other parameters are the same as in Fig. 6. Stable and unstable portions of the solution branches are marked by symbols "s" and "u" (in addition to the different colors). Arrows indicate stability borders.

azimuthal index of the infinitesimal perturbation, λ is the instability growth rate (which may be complex), and $*$ stands for the complex conjugation. The substitution of this expression in Eq. (1) leads to linearized equations,

$$(i\lambda + i\delta - k)f + \alpha f_{tt} + \rho[f_{rr} + r^{-1}f_r - r^{-2}(S+J)^2 f] + 2\eta|\psi|^2 f + \eta\psi^2 g + 3\omega|\psi|^4 f + 2\omega|\psi|^2\psi^2 g = 0, \quad (6)$$

$$(-i\lambda - i\delta - k)g + \alpha^* g_{tt} + \rho^*[g_{rr} + r^{-1}g_r - r^{-2}(S-J)^2 g] + 2\eta^*|\psi|^2 g + \eta^*(\psi^*)^2 f + 3\omega^*|\psi|^4 g + 2\omega^*|\psi|^2(\psi^*)^2 f = 0, \quad (7)$$

where $\alpha \equiv (D/2 - i\gamma)$, $\rho \equiv 1/2 - i\beta$, $\eta \equiv 1 - i\varepsilon$, and $\omega \equiv -\nu + i\mu$. Equations (6) and (7) are supplemented by boundary conditions demanding that the solutions vanish exponentially at $r \to \infty, |t| \to \infty$, and as $r^{|S+J|}$ and $r^{|S-J|}$ at $r \to 0$.

Results of the linear stability analysis are summarized in Figs. 8 and 9, where, fixing $\mu=1$, we vary the nonlinear gain ε and GVD coefficient D, and display the instability growth

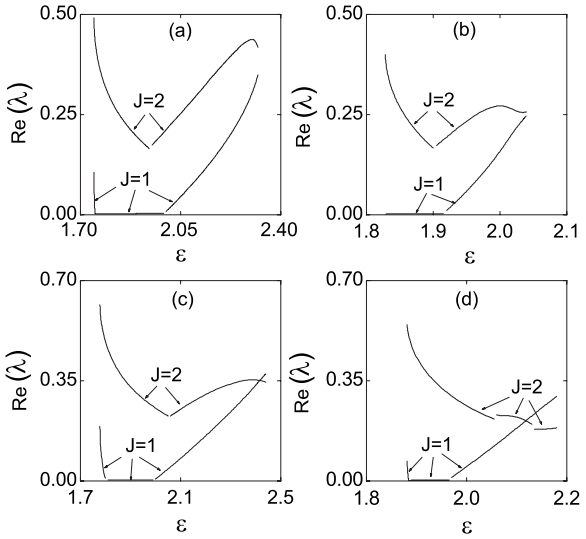

FIG. 8. The largest instability growth rate versus ε for spinning solitons with $S=1$ in the case of zero diffusivity, $\beta=0$. (a) $D=1$, $\nu=0.1$, (b) $D=-0.2$, $\nu=0.1$, (c) $D=1$, $\nu=0$, and (d) $D=-0.2$, $\nu=0$. Other parameters are $\mu=1$, $\gamma=0.5$, and $\delta=0.4$.

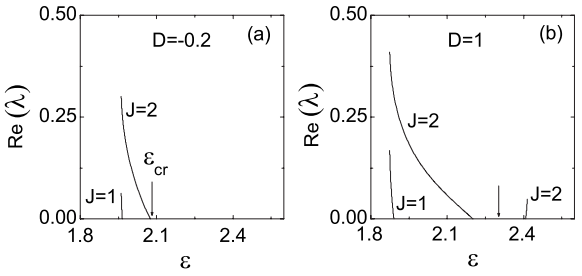

FIG. 9. The same as in Fig. 8 but for $\beta=0.1$ and $\nu=0.1$. (a) $D=-0.2$; (b) $D=1$. The other parameters are as in Fig. 7. The value of ε_{cr} is the stability border in (a); in (b), the arrow indicates the center of the stability interval, rather than its border.

rate, i.e., the largest value of Re(λ), found as the eigenvalue of Eqs. (6) and (7), versus ε for zero and nonzero diffusivity β. Figures 8 and 9 demonstrate that the perturbation with azimuthal index $J=2$ is the dominant one. In the case of $\beta=0$, the spinning solitons are unstable in the entire domain of their existence, as per Fig. 8. However, for $\beta>0$, stability domains for the spinning solitons are found, with both normal and anomalous GVD (in Ref. [45], only the case of anomalous GVD was investigated in detail). As mentioned above [see Figs. 7(a) and 7(b)], in the case of normal GVD there is a single stability border, marked by the vertical arrow in Fig. 9(a), whereas the stability interval has two borders in the case of anomalous GVD [the vertical arrow in Fig. 9(b) marks the center of the stability interval of the $S=1$ solitons].

The predictions of the linear stability analysis were verified in direct simulations of Eq. (1). To this end, initial conditions for a perturbed soliton were taken as $U(z=0)=\psi(r,t)(1+q\phi)\exp(iS\theta)$, where $\psi(r,t)$ is the stationary solution as per Eq. (4), q is a small perturbation amplitude, and ϕ is a random variable uniformly distributed in the interval of $[-0.5,0.5]$. In the simulations, it was observed that those perturbed spinning solitons which were predicted to be unstable either completely decay, or split into a set of spinless solitons, if slightly perturbed. Typical examples of the splitting of $S=1$ solitons (in both the normal- and anomalous-

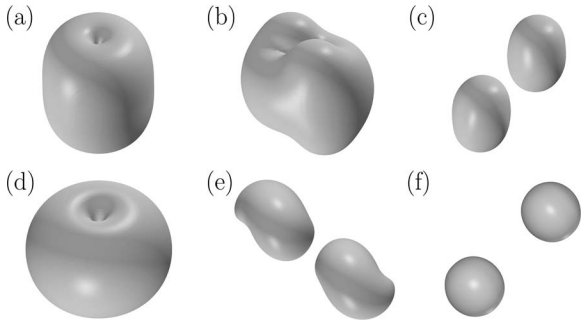

FIG. 10. (a)–(c) Isosurface plots illustrating the perturbation-induced splitting of unstable vortex tori (spinning solitons) with $S=1$, at $\beta=0$, $\varepsilon=2$, $\mu=1$, $\nu=0.1$, for normal GVD, $D=-0.2$. Panels (a), (b), and (c) display configurations at $z=0$, $z=420$, and $z=430$, respectively. (d)–(f) The same for the anomalous GVD, $D=1$, and $\varepsilon=1.9$. Panels (d), (e), and (f) pertain to $z=0$, $z=200$, and $z=205$, respectively. To plot this and the next figure, the simulations were performed on a 3D cubic grid with the linear size of $[-10.5,10.5]$.

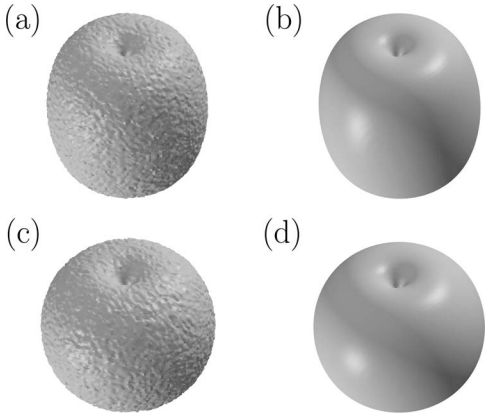

FIG. 11. (a), (b) The recovery of a perturbed stable spinning soliton with $S=1$, at $\beta=0.1$, $\mu=1$, and $\nu=0.1$, in the case of normal GVD, with $D=-0.2$ and $\varepsilon=2.1$. Panels (a) and (b) show the shape of the vortex torus at $z=0$ and $z=300$, respectively. (c), (d) The same in the case of anomalous GVD, with $D=1$ and $\varepsilon=2.3$.

GVD regimes) into two pulses with $S=0$ due to the azimuthal instability are shown in Fig. 10. The outcome agrees with the fact that the strongest instability mode for these solitons is, pursuant to Fig. 8, the one with $J=2$; hence it should indeed split into two fragments.

It has also been verified that those spinning solitons (with $S=1$) which were predicted above to be linearly stable are indeed stable against the addition of finite random perturbations. Examples of self-healing of stable spinning solitons with the initial relative perturbation amplitude at the level of 10% are displayed in Fig. 11, for the normal and anomalous GVD in parallel.

IV. CONCLUSIONS

In this work, we have expanded the studies of 3D dissipative vortex solitons with the toroidal shape in the complex Ginzburg-Landau equation with the cubic-quintic nonlinearity, which were recently initiated in Ref. [45]. The cubic-quintic complex Ginzburg-Landau equation provides for a model of dispersive bulk optical media with saturable self-focusing nonlinearity, nonlinear gain, and spectral filtering. An important issue is the dependence of the stability of the vortex solitons on physical parameters. In Ref. [45], it was found that the saturation of the self-focusing Kerr nonlinearity is not an essential condition for the stability of fundamental and vortex solitons, as the supercritical collapse induced by the Kerr nonlinearity in the 3D medium may be effectively suppressed by the dissipative part of the model. However, the role of the effective diffusivity in the transverse plane, and of the sign of the group-velocity dispersion in the longitudinal (temporal) direction—anomalous or normal—remained unknown. In this work, using the accurate linear-stability analysis and direct simulations of perturbed solitons, we have found that the diffusivity is necessary for the stability of the vortex solitons against splitting (while zero-vorticity solitons may be stable in the absence of the diffusivity). On the other hand, stable dissipative solitons, with zero and nonzero vorticity alike, exist with both anomalous

and normal group-velocity dispersion, the stability region of dissipative solitons with nonzero vorticity being *wider* in the latter case.

It has also been found that, at values of the nonlinear gain above the upper border of their existence region, the three-dimensional dissipative solitons either develop intrinsic pulsations (regular or multiple-periodic ones, in the cases of the normal and anomalous group-velocity dispersion, respectively), or start expansion in the temporal (longitudinal) direction, keeping the fixed structure in the transverse plane. The latter effect may be used, in principle, to grow photonic channels and multichannel arrays in bulk optical media.

ACKNOWLEDGMENT

This work was supported, in part, by the Deutsche Forschungsgemeinschaft (DFG), Bonn.

[1] A. C. Newell, *Solitons in Mathematics and Physics* (SIAM, Philadelphia, 1985).
[2] N. N. Akhmediev and A. Ankiewicz, *Solitons: Nonlinear Pulses and Beams* (Chapman & Hall, London, 1997).
[3] G. I. Stegeman and M. Segev, Science **286**, 1518 (1999).
[4] G. I. Stegeman, D. N. Christodoulides, and M. Segev, IEEE J. Sel. Top. Quantum Electron. **6**, 1419 (2000).
[5] Yu. S. Kivshar and G. P. Agrawal, *Optical Solitons: From Fibers to Photonic Crystals* (Academic, San Diego, 2003).
[6] B. A. Malomed, D. Mihalache, F. Wise, and L. Torner, J. Opt. B: Quantum Semiclassical Opt. **7**, R53 (2005).
[7] B. A. Malomed, *Soliton Management in Periodic Systems* (Springer, New York, 2006).
[8] *Dissipative Solitons*, edited by N. Akhmediev and A. Ankiewicz, Lecture Notes in Physics Vol. 661 (Springer, Berlin, 2005).
[9] S. Barland, J. R. Tredicce, M. Brambilla, L. A. Lugiato, S. Balle, M. Giudici, T. Maggipinto, L. Spinelli, G. Tissoni, T. Knodl, M. Miller, and R. Jager, Nature (London) **419**, 699 (2002); Z. Bakonyi, D. Michaelis, U. Peschel, G. Onishchukov, and F. Lederer, J. Opt. Soc. Am. B **19**, 487 (2002); E. A. Ultanir, G. I. Stegeman, D. Michaelis, C. H. Lange, and F. Lederer, Phys. Rev. Lett. **90**, 253903 (2003).
[10] N. N. Rosanov, *Spatial Hysteresis and Optical Patterns* (Springer, Berlin, 2002).
[11] C. Elphick and E. Meron, Phys. Rev. A **40**, 3226 (1989); I. V. Barashenkov, M. M. Bogdan, and V. I. Korobov, Europhys. Lett. **15**, 113 (1991); M. Bondila, I. V. Barashenkov, and M. M. Bogdan, Physica D **87**, 314 (1995); S. Longhi, G. Steinmeyer, and W. S. Wong, J. Opt. Soc. Am. B **14**, 2167 (1997).
[12] J. Atai and B. A. Malomed, Phys. Lett. A **246**, 412 (1998); H. Sakaguchi and B. A. Malomed, Physica D **147**, 273 (2000).
[13] N. R. Pereira and L. Stenflo, Phys. Fluids **20**, 1733 (1977).
[14] M. C. Cross and P. C. Hohenberg, Rev. Mod. Phys. **65**, 851 (1993).
[15] I. Aranson and L. Kramer, Rev. Mod. Phys. **74**, 99 (2002); B. A. Malomed, in *Encyclopedia of Nonlinear Science*, edited by A. Scott (Routledge, New York, 2005), p. 157.
[16] P. Manneville, *Dissipative Structures and Weak Turbulence* (Academic, San Diego, 1990).
[17] P. Mandel and M. Tlidi, J. Opt. B: Quantum Semiclassical Opt. **6**, R60 (2004).
[18] H. A. Haus, J. G. Fujimoto, and E. P. Ippen, J. Opt. Soc. Am. B **8**, 2068 (1991); P. K. Jakobsen, J. V. Moloney, A. C. Newell, and R. Indik, Phys. Rev. A **45**, 8129 (1992); J. D. Moores, Opt. Commun. **96**, 65 (1993).
[19] L. M. Hocking and K. Stewartson, Proc. R. Soc. London, Ser. A **326**, 289 (1972); P. Kolodner, Phys. Rev. A **44**, 6466 (1991).
[20] P. A. Bélanger, L. Gagnon, and C. Paré, Opt. Lett. **14**, 043 (1989); G. P. Agrawal, Phys. Rev. A **44**, 7493 (1991); B. A. Malomed, M. Gölles, I. M. Uzunov, and F. Lederer, Phys. Scr. **55**, 73 (1997); B. A. Malomed, A. G. Vladimirov, G. V. Khodova, and N. N. Rosanov, Phys. Lett. A **274**, 111 (2000).
[21] H. Leblond, A. Komarov, M. Salhi, A. Haboucha, and F. Sanchez, J. Opt. A, Pure Appl. Opt. **8**, 319 (2006).
[22] E. N. Tsoy, A. Ankiewicz, and N. Akhmediev, Phys. Rev. E **73**, 036621 (2006).
[23] K. Nozaki and N. Bekki, J. Phys. Soc. Jpn. **53**, 1581 (1984); R. Conte and M. Musette, Physica D **69**, 1 (1993); D. Anderson, F. Cattani, and M. Lisak, Phys. Scr., T **82**, 32 (1999).
[24] B. A. Malomed and H. G. Winful, Phys. Rev. E **53**, 5365 (1996); J. Atai and B. A. Malomed, *ibid.* **54**, 4371 (1996); Phys. Lett. A **246**, 412 (1998).
[25] H. Michinel, M. J. Paz-Alonso, and V. M. Pérez-García, Phys. Rev. Lett. **96**, 023903 (2006).
[26] V. I. Petviashvili and A. M. Sergeev, Dokl. Akad. Nauk SSSR **276**, 1380 (1984) [Sov. Phys. Dokl. **29**, 493 (1984)].
[27] B. A. Malomed, Physica D **29**, 155 (1987) (see Appendix in this paper); O. Thual and S. Fauve, J. Phys. (Paris) **49**, 1829 (1988); S. Fauve and O. Thual, Phys. Rev. Lett. **64**, 282 (1990).
[28] W. van Saarloos and P. C. Hohenberg, Phys. Rev. Lett. **64**, 749 (1990); V. Hakim, P. Jakobsen, and Y. Pomeau, Europhys. Lett. **11**, 19 (1990); B. A. Malomed and A. A. Nepomnyashchy, Phys. Rev. A **42**, 6009 (1990); P. Marcq, H. Chaté, and R. Conte, Physica D **73**, 305 (1994).
[29] N. Akhmediev and V. V. Afanasjev, Phys. Rev. Lett. **75**, 2320 (1995).
[30] H. R. Brand and R. J. Deissler, Phys. Rev. Lett. **63**, 2801 (1989); R. J. Deissler and H. R. Brand, *ibid.* **72**, 478 (1994); **74**, 4847 (1995); **81**, 3856 (1998).
[31] V. V. Afanasjev, N. Akhmediev, and J. M. Soto-Crespo, Phys. Rev. E **53**, 1931 (1996).
[32] J. M. Soto-Crespo, N. Akhmediev, and A. Ankiewicz, Phys. Rev. Lett. **85**, 2937 (2000); J. M. Soto-Crespo and N. Akhmediev, Math. Comput. Simul. **69**, 526 (2005).
[33] W. Chang, A. Ankiewicz, and N. Akhmediev, Phys. Lett. A **362**, 31 (2007).
[34] L.-C. Crasovan, B. A. Malomed, and D. Mihalache, Phys. Rev. E **63**, 016605 (2001); Phys. Lett. A **289**, 59 (2001).
[35] P. Grelu, J. M. Soto-Crespo, and N. Akhmediev, Opt. Express

13, 9352 (2005).
[36] J. M. Soto-Crespo, P. Grelu, and N. Akhmediev, Opt. Express **14**, 4013 (2006).
[37] N. Efremidis, K. Hizanidis, B. A. Malomed, H. E. Nistazakis, and D. J. Frantzeskakis, J. Opt. Soc. Am. B **17**, 952 (2000).
[38] L.-C. Crasovan, Y. V. Kartashov, D. Mihalache, L. Torner, Y. S. Kivshar, and V. M. Pérez-García, Phys. Rev. E **67**, 046610 (2003).
[39] A. S. Desyatnikov, Y. S. Kivshar, and L. Torner, Prog. Opt. **47**, 291 (2005).
[40] D. Mihalache, D. Mazilu, L. C. Crasovan, I. Towers, A. V. Buryak, B. A. Malomed, L. Torner, J. P. Torres, and F. Lederer, Phys. Rev. Lett. **88**, 073902 (2002); D. Mihalache, D. Mazilu, L. C. Crasovan, I. Towers, B. A. Malomed, A. V. Buryak, L. Torner, and F. Lederer, Phys. Rev. E **66**, 016613 (2002).
[41] S. K. Adhikari, Phys. Rev. E **65**, 016703 (2001); H. Saito and M. Ueda, Phys. Rev. Lett. **89**, 190402 (2002); L. Salasnich, Laser Phys. **14**, 291 (2004); D. Mihalache, D. Mazilu, B. A. Malomed, and F. Lederer, Phys. Rev. A **73**, 043615 (2006); L. D. Carr and C. W. Clark, Phys. Rev. Lett. **97**, 010403 (2006); B. A. Malomed, F. Lederer, D. Mazilu, and D. Mihalache, Phys. Lett. A **361**, 336 (2007).
[42] P. G. Kevrekidis, B. A. Malomed, D. J. Frantzeskakis, and R. Carretero-González, Phys. Rev. Lett. **93**, 080403 (2004); R. Carretero-González, P. G. Kevrekidis, B. A. Malomed, and D. J. Frantzeskakis, *ibid.* **94**, 203901 (2005).
[43] M. Quiroga-Teixeiro and H. Michinel, J. Opt. Soc. Am. B **14**, 2004 (1997).
[44] I. Towers, A. V. Buryak, R. A. Sammut, B. A. Malomed, L.-C. Crasovan, and D. Mihalache, Phys. Lett. A **288**, 292 (2001); R. L. Pego and H. A. Warchall, J. Nonlinear Sci. **12**, 347 (2002); B. A. Malomed, L.-C. Crasovan, and D. Mihalache, Physica D **161**, 187 (2002).
[45] D. Mihalache, D. Mazilu, F. Lederer, Y. V. Kartashov, L.-C. Crasovan, L. Torner, and B. A. Malomed, Phys. Rev. Lett. **97**, 073904 (2006).
[46] V. Skarka and N. B. Aleksić, Phys. Rev. Lett. **96**, 013903 (2006).
[47] J. M. Soto-Crespo, N. Akhmediev, and Ph. Grelu, Phys. Rev. E **74**, 046612 (2006).
[48] H. Sakaguchi, Physica D **210**, 138 (2005).
[49] H. Sakaguchi and B. A. Malomed, Physica D **167**, 123 (2002).
[50] S. Skupin, L. Bergé, U. Peschel, F. Lederer, G. Méjean, J. Yu, J. Kasparian, E. Salmon, J. P. Wolf, M. Rodriguez, L. Wöste, R. Bourayou, and R. Sauerbrey, Phys. Rev. E **70**, 046602 (2004).
[51] P. Coullet, L. Gil, and F. Rocca, Opt. Commun. **73**, 403 (1989).
[52] J. Lega, J. V. Moloney, and A. C. Newell, Phys. Rev. Lett. **73**, 2978 (1994).
[53] J. Lega, J. V. Moloney, and A. C. Newell, Physica D **83**, 478 (1995).
[54] A. Komarov, H. Leblond, and F. Sanchez, Phys. Rev. E **72**, 025604(R) (2005).